Three-Dimensional Electron Microscopy of Human Umbilical Cord Tissue Allograft Pre and Post Processing: A Literature Comparison

Joseph R Purita[1], John Shou[2], Naomi Lambert[2], Justine Davis[2], Tyler Barrett[2]
[1]Institute of Regenerative Medicine, [2]Regenative Labs

Regenative LABS

MONTANA STATE UNIVERSITY

Abstract

One in four adults in the US suffer from cartilage degeneration of the Intervertebral Disc (DDD) or load-bearing joints (DJD). Since cartilage is avascular, it has a limited regenerative capacity. Conventional non-surgical treatments provide brief symptomatic relief, have side effects, and do not address the cartilage defect itself. As such, new alternatives are needed. Perinatal birth tissue allografts are a novel frontier for bio-mechanical cartilage engineering research. The tissues of interest include umbilical cord-derived Wharton's Jelly (WJ). This study assessed WJ tissue samples via ZEISS Supra 55VP Field Emission Scanning Electron Microscope (SEM) at 100 and 300 nm resolution scales. The captured images of pre and post-processed structural tissue matrices in WJ allografts were analyzed against themselves and peer-reviewed SEM images of articular cartilage, intervertebral disc cartilage, and muscle fascia. SEM images of post-processed WJ structural tissue matrices were found to be comparable to structural tissue matrices in human articular cartilage, intervertebral disc cartilage, and muscle fascia on a qualitative and quantitative level. This is the first study that we are aware of, to demonstrate that the structural collagen matrix in post-processed WJ allografts are analogous in structure to the cartilage in articular joints, intervertebral discs, and muscle fascia.

Introduction

- WJ spans the entire length of the umbilical cord, located between the blood vessels of the umbilical cord and the amniotic epithelium, providing protection, cushioning, and structural support [2,3]
- WJ contains cytokines, growth factors, proteoglycans, hyaluronic acid, the biomechanical microarchitecture for collagen extracellular matrix [4]
- ECM is a collagen-based, cross-linked network that provides tensile strength and distributes load. Damage, degeneration or diminished function in collagen cross-bridging will lead to loss of mechanical properties of the collagen network [5]
- Collagen-specific structural tissue defects can be identified by physical examination and confirmed with MRI or musculoskeletal ultrasound
- Human tissue strength is directly dependent upon the sizeable crosslinking of collagen [9]. Collagen types II, III, V, VI, and XII have been isolated from WJ [2,10].
- Current research demonstrates that WJ exerts an effect independent of any cellular activity [3]
- This study aimed to assess WJ tissue samples via a ZEISS Supra 55VP Field Emission Scanning Electron Microscope (SEM) at 100 and 300 nm resolution scales

Methods and Materials

All methods were completed in compliance with the FDA and American Association of Tissue Banks (AATB) standards.

Donation and Collection. Human umbilical cords were obtained from consenting donors following full-term Cesarean section deliveries. Prior to delivery, donors underwent comprehensive medical, social, and blood testing. All donations were tested for infectious disease in accordance with Clinical Laboratory Improvement Amendments (CLIA) of 1988, 42 CFR part 493, and FDA regulations. Each test was performed with an FDA-Approved testing kit [See Appendix A]. All test results were negative or non-reactive.

Preparation of the Pre-Processed Umbilical Cord Tissue Samples. All procedures were performed in accordance with strict aseptic technique. In an ISO class 5 biologic safety cabinet, the umbilical cord was rinsed with saline to remove excess blood residue and clots. Various sized cross-sections of the umbilical cord were cut and placed on a sterile drying tray. The cross-sections were then desiccated in a high nitrogen concentration drying chamber.

Preparation of Processed Umbilical Cord Tissue Samples Product. Wharton's jelly was aseptically dissociated from the rinsed umbilical cord. After dissociation, 150mg of Wharton's Jelly was suspended in approximately 2 mL of sterile Sodium Chloride 0.9% solution (normal saline). The sample was not combined with cells, tissues, or any other articles save the exceptions outlined in 21 CFR Part 1271.10(a)(3) (Human Cells, Tissues, and Cellular and Tissue-Based Product Regulation). The manufacture of the HCT/P does not involve the combination of the cells or tissues with another article, except for water, crystalloids, or a sterilizing, preserving, or storage agent, provided that the addition of water, crystalloids, or the sterilizing, preserving, or storage agent does not raise new clinical safety concerns with the respect to the HCT/P15. Scanning Electron Microscope Imaging. Pre-processed and post-processed desiccated tissue samples were received by the University of Montana laboratory for analysis and electron microscope imaging. The tissue samples were transferred to a sticky carbon surface (PELCO Tab, Ted Pella, Inc.) and coated with a thin layer of iridium (60 seconds at 25 mA, Emite K575X Sputter Coater) to mitigate charging in the microscope. The tissue samples were then examined via a ZEISS Supra 55VP Field-Emission Scanning Electron Microscope (SEM) at a 100 and 300 nm scale of resolution.

Results

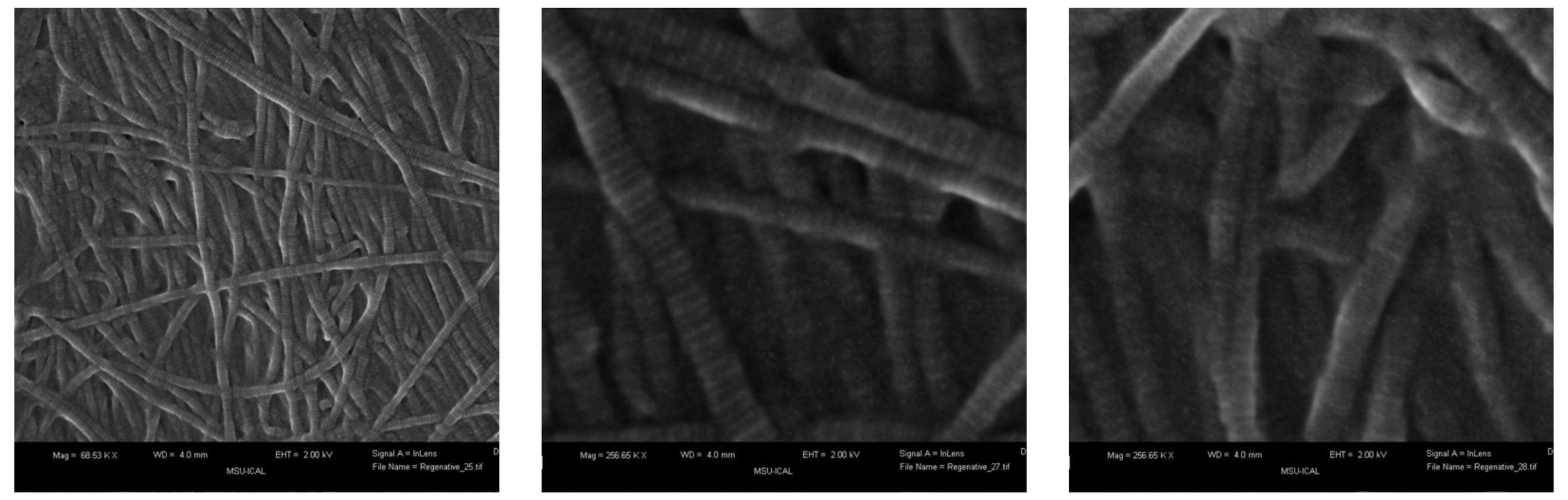

Figure 1. SEM micrographs of pre-processed umbilical cord tissue samples. (A) SEM image of cross-linked collagen structures. (scale bar: 300nm) (B) SEM image of collagenic structure fibers. (scale bar: 100nm) (C) SEM image of collagenic structure fibers (scale bar: 100nm).

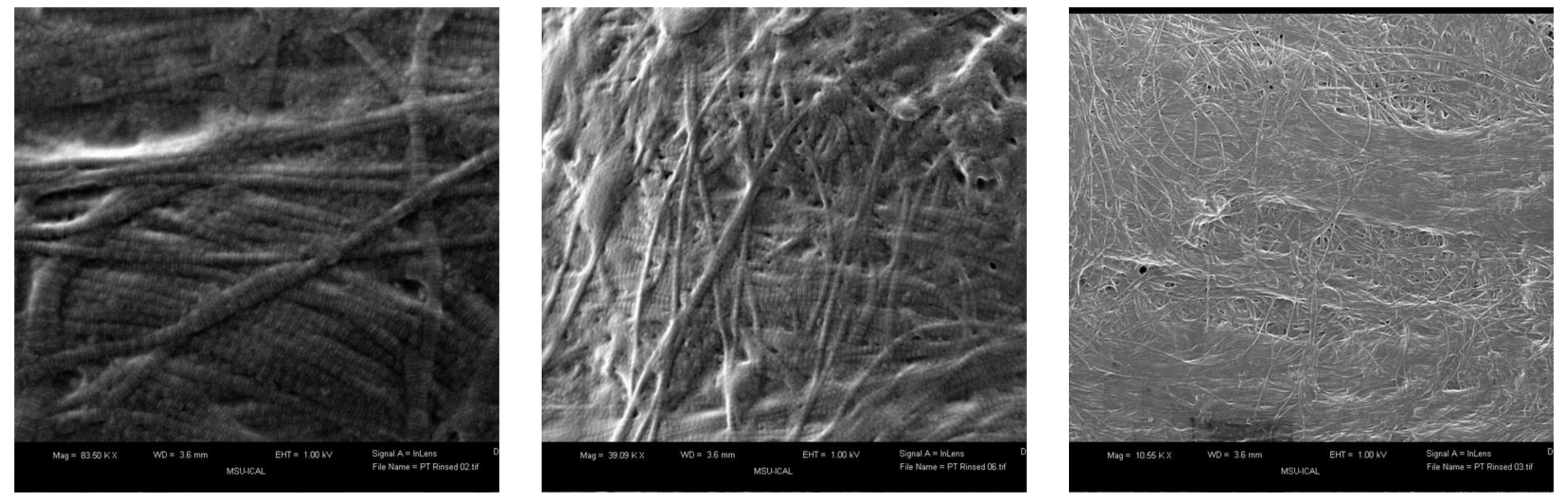

Figure 2. SEM micrographs of post-processed umbilical cord tissue samples. (A) SEM image of preserved cross-linked collagen structures. (scale bar: 300 nm) (B) SEM image of preserved random directional structural composition of collagen fibers. (scale bar: 300 nm) (C) SEM image of multidirectional linkage of collagen fibers (scale bar: 1μm).

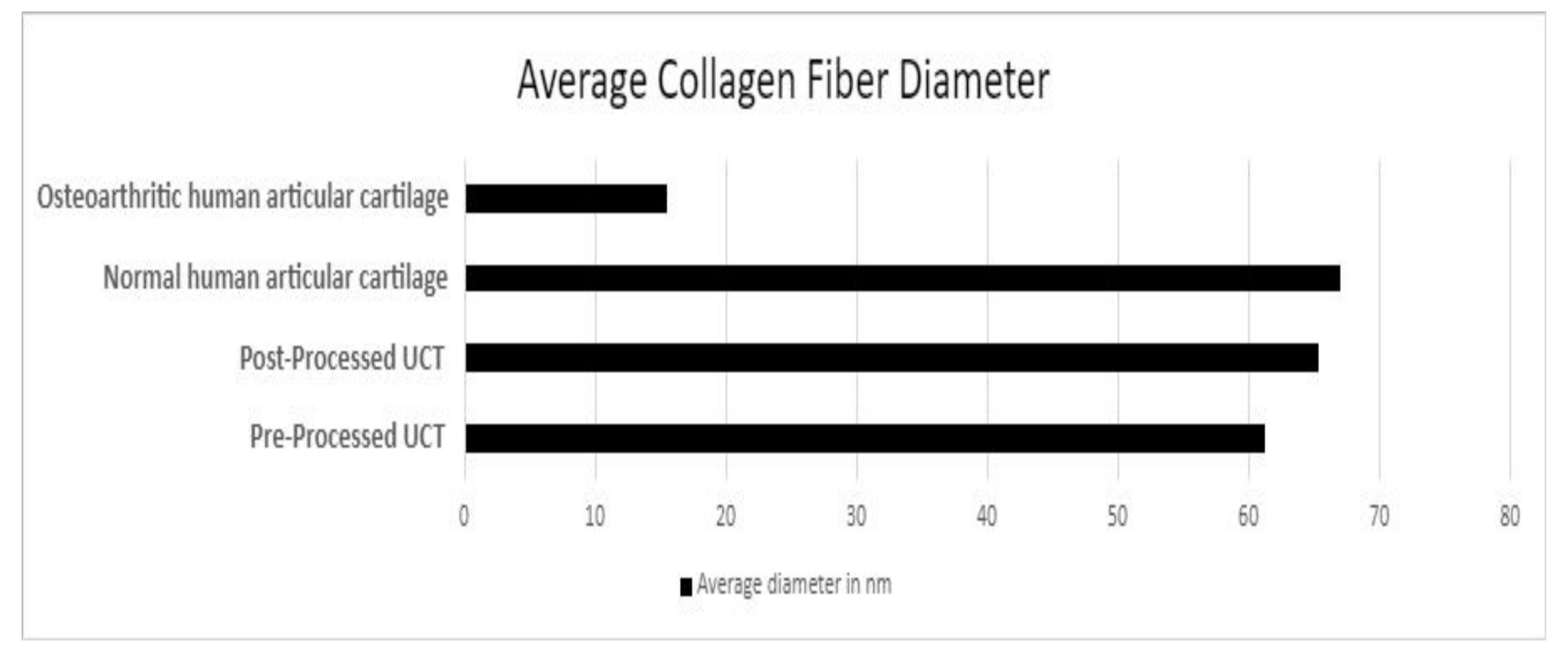

Figure 5. Fiber diameters were determined from SEM photos of post and pre-processed UCT tissues and compared with diameters found in the Supramolecular Organization of Collagen Fibrils in Healthy and Osteoarthritic Human Knee and Hip Joint Cartilage study.

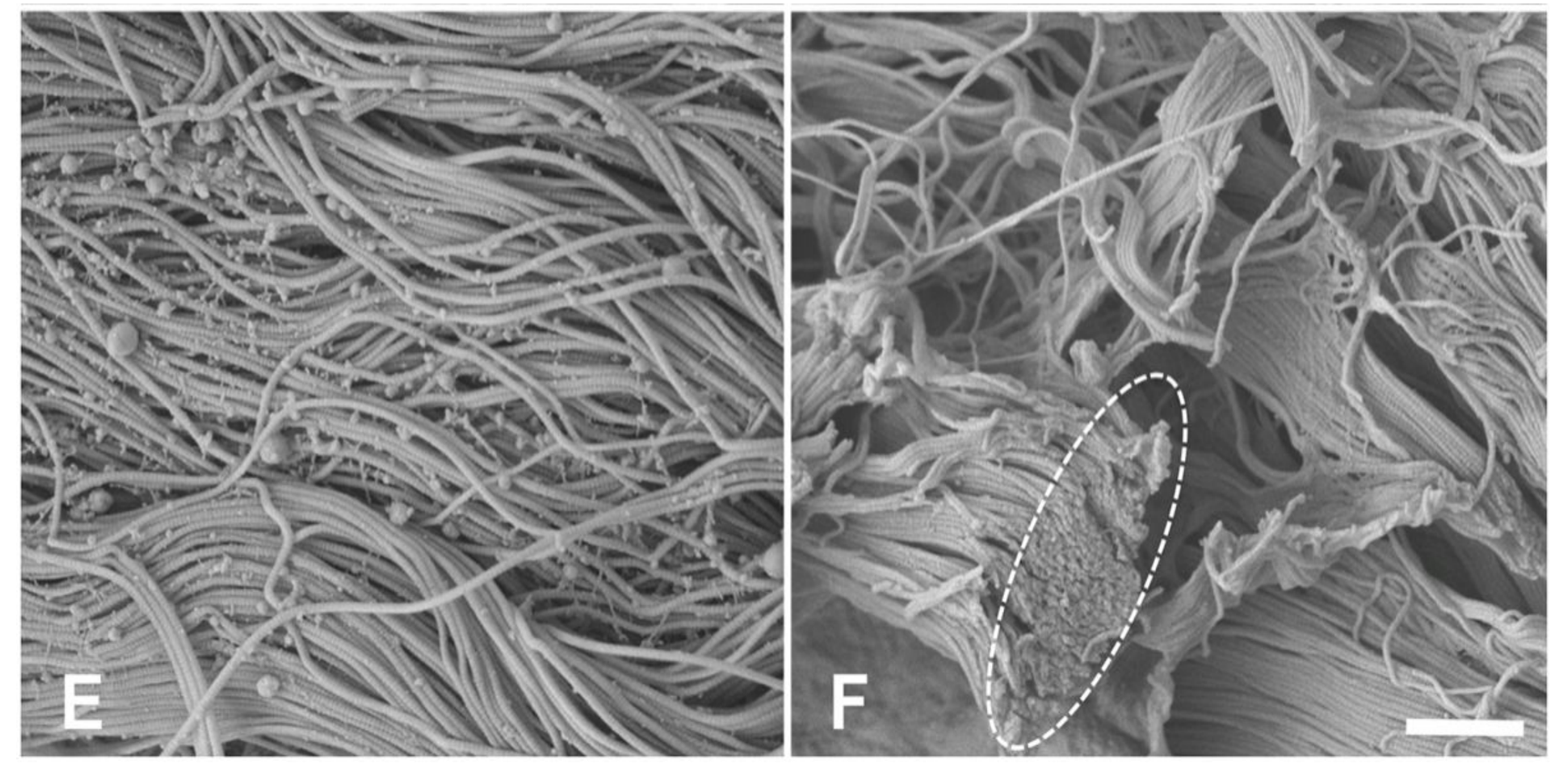

Figure 7. Scanning electron microscopy of native skin. In the higher 10,000x magnification type I collagen clotting was observed (interrupted circles) accompanied by a loss of cross-linking collagens. Scale bar 1 μm. The mean collagen fiber diameter from papillary and reticular dermis in normal skin was 56.2 +/- 2.5 nm and 62.8 +/- 4.3 nm respectively

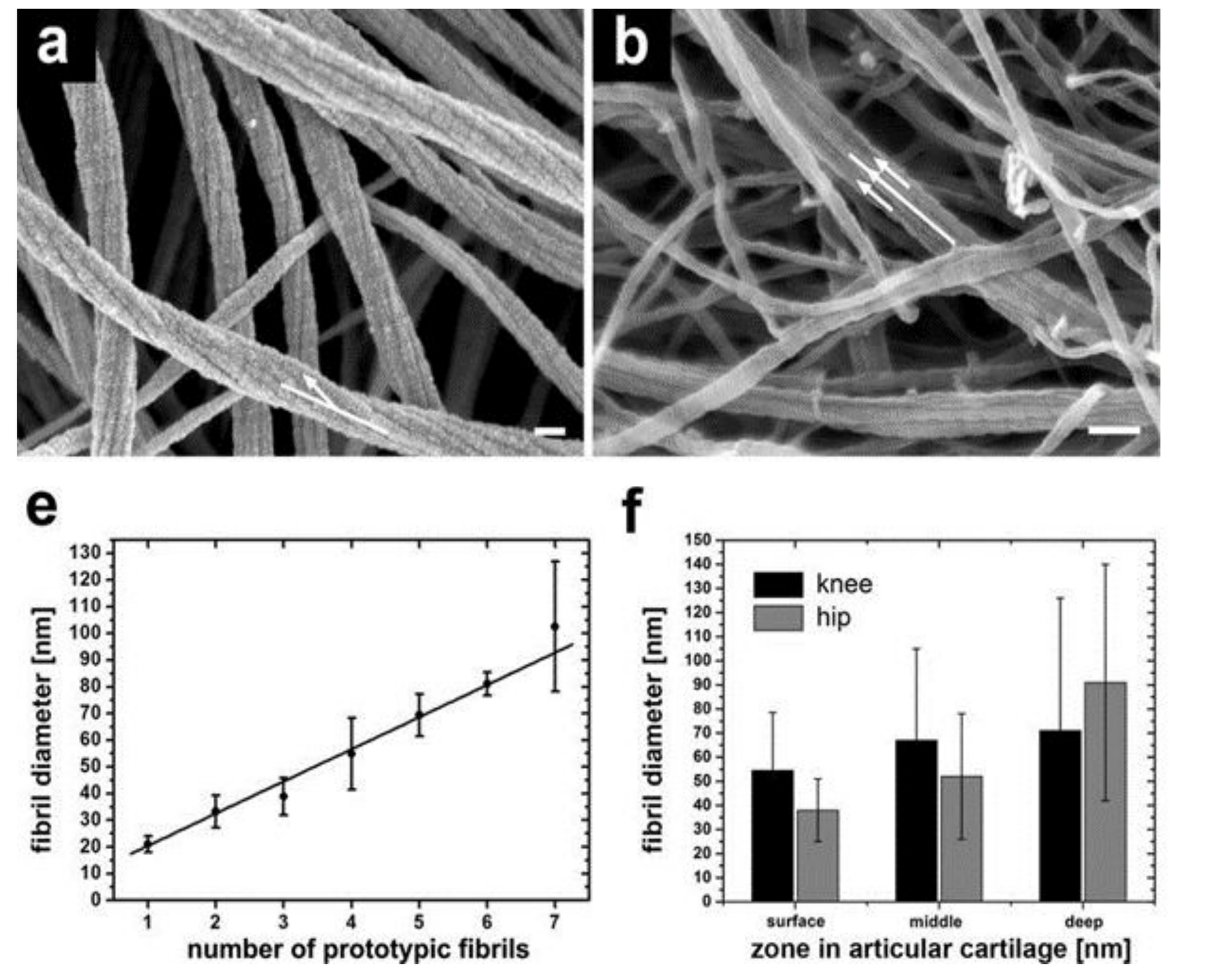

Figure 3. Literature comparison of SEM images of normal human articular cartilage after enzymatic depletion of the proteoglycan moiety and chondrocytes. (a) SEM image of the collagen fiber meshwork from knee surface articular cartilage shows (i) the 67 nm D-band periodicity,(iii) a twisting of the prototypic fibril along the long axis of roughly about 400 nm (white arrow). (b) SEM image of hip surface articular cartilage with untwisted fibers (white arrows).(e) Graph shows the increase of collagen fiber diameter with the number of prototypic fibrils. (f) Comparison between fiber diameters in each zone in hip articular cartilage and knee articular cartilage. Scale bars, 100 nm (a to d).

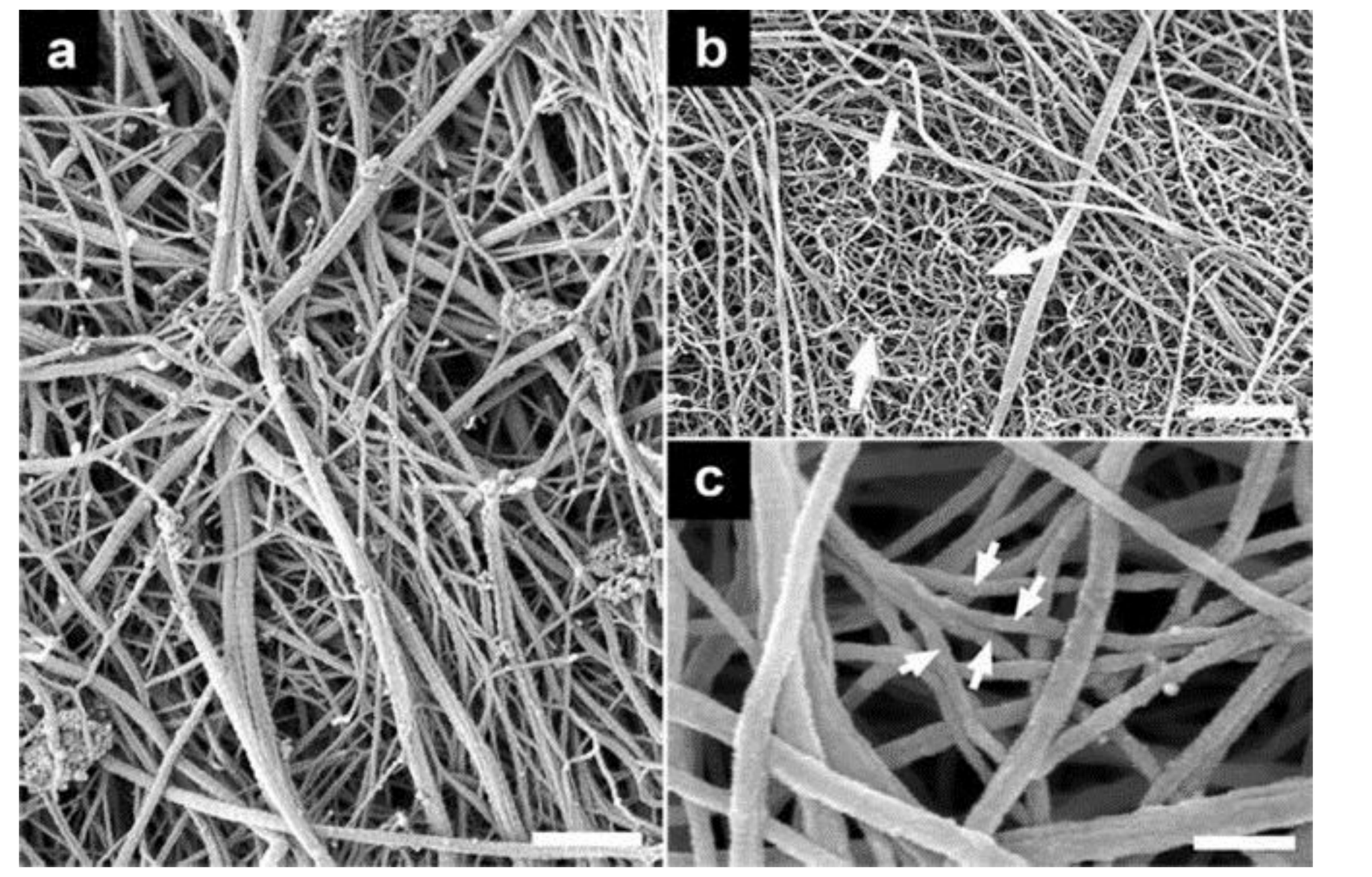

Figure 4. Literature comparison of SEM images illustrating articular cartilage in osteoarthritic patients. SEM image of grade 3 osteoarthritic cartilage (knee) (a) breakdown of thicker collagen fibers with a diameter of 40–60 nm into thinner fibers down to bundles made of only one prototypic fibril of 18 ± 5 nm in diameter. (b) end-stage of fiber breakdown, that is a wool-like structure (white arrows) with filaments exhibiting a diameter of d = 13 ± 2 nm. (c) Degrading articular cartilage larger fibers split into smaller sized fibrils that are often arranged as a highly entangled fibrillar meshwork (white arrows). Scale bars, 500 nm (a and c); 100 nm

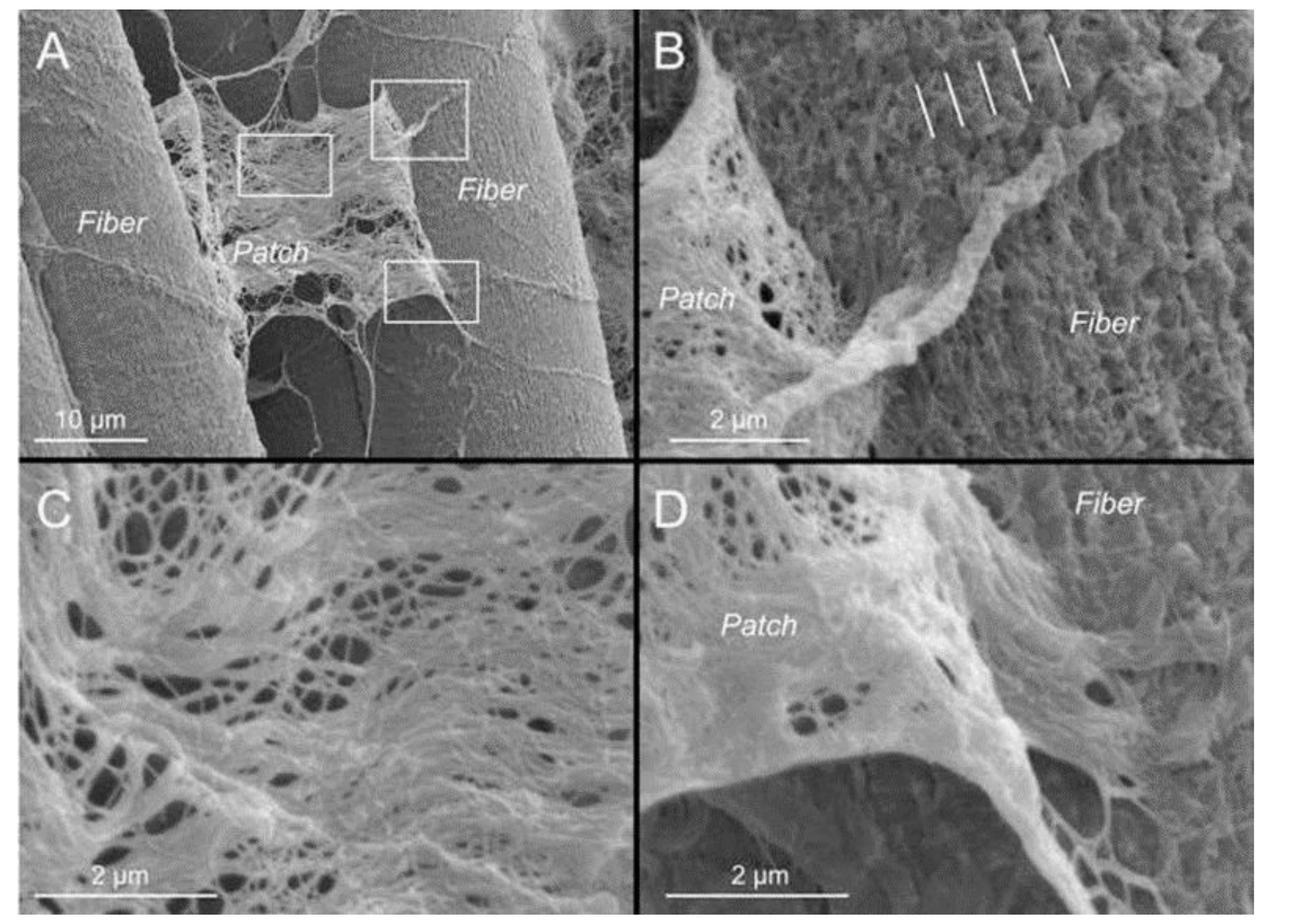

Figure 6. Literature comparison of SEM images illustrating collagen presence in skeletal muscle collagen types II, III, V, VI, and XII have been isolated from WJ. (A) Sections of ECM separated from muscle fibers during sample preparation. Sections are represented by white rectangles. (scale bar: 10μm) (B) Longitudinal ECM organization is seen on the fiber surface, as noted by the rectangular lines. (scale bar: 2μm) (C) Collagen fibril network organization observed through the central region of an ECM patch. (scale bar: 2μm) (D) ECM patch appears firmly connected to the skeletal muscle fiber surface. (scale bar: 2 μm

Discussion

In the current study, WJ allografts were produced through minimal manipulation of human umbilical cord tissue samples and are denoted as post-processed umbilical cord tissues. It is evident when comparing Figures 1 and 2 that the structural properties of the WJ before and after processing have been retained and are consistent with FDA guidelines defining minimal manipulation of WJ allografts. The diameter of the UCT fibers increased from approximately 61nm pre-processing to 65 nm post-processing. This increase could be due to slight swelling from the saline rinse and is not statistically significant. The average diameter of healthy mid-zone articular cartilage is around 67 nm (Figure 3), similar in size and formation to the processed WJ (Figure 5). This characteristic further confirms minimal manipulation of pre- and post-processed tissue. Collagen is the most prevalent structural macromolecule within the extracellular matrix, arranged in a cross-fiber network [14-16]. The strategic linkage of collagen fibers allows the network to provide protection, cushioning, and structural support, identical to the role of WJ in the umbilical cord[12]. The structure of the collagen fibers remains intact after processing, affording the WJ allograft the intended function of providing cushioning and structural support to the site of the structural tissue defect [17,18].

The multidirectional collagen network observed in WJ appears to be structurally comparative to the collagenic organization found in the extracellular matrix of cartilage [16,19]. Previously published research indicates that WJ may demonstrate chondrogenic differentiation capabilities, which could be beneficial in cartilage regeneration [19]. The anatomic structural similarities between different collagen networks (Figures 3, 6, 7) indicate that human umbilical cord tissue allografts are comparatively homologous in structure to the extracellular matrix found in cartilage and dermis. The breakdown of collagen (Figure 4C) results in the deterioration of cartilage [8]. Patients with structural tissue defects typically experience impairments in functional outcomes and quality of life. While applications of human umbilical cord tissue allografts have been used extensively in the clinical treatment of cartilage tears, there is also potential for allografts to be used in the pathology of intervertebral discs, as well as muscle tears, and deep tunneling wounds [20]. As a nonsurgical option, applying homologous WJ tissue allografts to structural tissue defects warrants clinical consideration.

Despite WJ being a non-vascular, dense irregular connective tissue, there is also the promise of homologous applications for WJ in vascularized tissue. In figure 6C, the organization of the collagen fibril network in skeletal muscle closely resembles the multidirectional collagen fibers seen in the post-processed umbilical cord tissue samples (Figure 2). The extracellular matrix of skeletal muscles comprises a three-dimensional architecture consisting primarily of collagen, glycoproteins, and elastin [21]. Forty percent of the human body weight is composed of skeletal muscle [22]. The application of WJ as a homologous allograft in patients with structural tissue defects in skeletal muscle provides an opportunity for future observational and prospective clinical studies. The clinical applications of human umbilical cord tissue allografts are profound in both vascularized and non-vascularized structural defects. The utilization of umbilical cord tissue allografts in regenerative medicine will be continually enhanced with additional discoveries of homologous use applications in clinical research data.

Conclusions

Through observational, collagenic structural comparison from SEM images, WJ demonstrates the potential to be used as an architectural scaffold for ECM supplementation in cartilage-based tissue structures and skeletal muscle tears. Even after processing, WJ retained its pre-processing structural characteristics. Further, the SEM images demonstrate comparative microarchitectural characteristics in post-processing WJ samples and ECM in articular cartilage and peri-muscle fiber fascia. The shared SEM characteristics are consistent between both tissue types, supporting homologous use.

Future Directions

In future work, we intend to use proteomic analysis of collagen fibers to confirm the anatomical comparison between human umbilical cord tissue allografts, skeletal muscle, and cartilage. This analysis would be coupled with high-resolution confocal antibody staining of umbilical cord tissue to allow for differentiation between the different types of collagen in the extracellular matrix. Future case studies documenting umbilical cord tissue allograft efficacy could include applications in orthopedics, gerontology, sports medicine, general family medicine, and operating rooms. These advancements and commercial coverage of WJ allografts would increase physician and patient access to commercially available umbilical cord tissue allografts. Ease of access to perinatal birth tissue allografts like Wharton's Jelly could dramatically improve community health, and reduce global surgical healthcare costs.

Institutional Review Board Statement

The study was conducted in accordance with the Declaration of Helsinki, and approved by the Institutional Review Board of the Institute of Regenerative and Cellular Medicine (protocol code IRCM-2022-311 and approved on 12 January 2022).

References

1. Kim DW, Staples M, Shinozuka K, Pantcheva P, Kang SD, Borlongan CV. Wharton's jellyderived mesenchymal stem cells: phenotypic characterization and optimizing their therapeutic potential for clinical applications. Int J Mol Sci. 2013 May 31;14(6):11692-712. doi: 10.3390/ijms140611692. PMID: 23727936; PMCID: PMC3709752.
2. Gupta A, El-Amin SF 3rd, Levy HJ, Sze-Tu R, Ibim SE, Maffulli N. Umbilical cordderived Wharton's jelly for regenerative medicine applications. J Orthop Surg Res. 2020 Feb 13;15(1):49. doi: 10.1186/s13018-020-1553-7. PMID: 32054483; PMCID: PMC7017504.
3. Deus IA, Mano JF, Custódio CA. Perinatal tissues and cells in tissue engineering and regenerative medicine. Acta Biomater. 2020 Jul 1;110:1-14. doi: 10.1016/j. actbio.2020.04.035. Epub 2020 May 14. PMID: 32418650.
4. Jadalannagari S, Converse G, McFall C, Buse E, Filla M, Villar MT, Artigues A, Mellot AJ, Wang J, Detamore MS, Hopkins RA, Aljitawi OS. Decellularized Wharton's Jelly from human umbilical cord as a novel 3D scaffolding material for tissue engineering applications. PLoS One. 2017 Feb 21;12(2):e0172098. doi: 10.1371/journal. pone.0172098. Erratum in: PLoS One. 2017 Mar 7;12 (3):e0173827. PMID: 28222169; PMCID: PMC5319682.
5. Feng H, Danfelter M, Strömqvist B, Heinegård D. Extracellular matrix in disc degeneration. J Bone Joint Surg Am. 2006 Apr;88 Suppl 2:25-9. doi: 10.2106/ JBJS.E.01341. PMID: 16595439.
6. Mureşan S, Mureşan M, Voidăzan S, Neagoe R. The accuracy of musculoskeletal ultrasound examination for the exploration of meniscus injuries in athletes. J Sports Med Phys Fitness. 2017 May;57(5):589-594. doi: 10.23736/S0022-4707.17.06132-1. Epub 2015 Dec 18. PMID: 26684438.
7. Luo Y, Sinkeviciute D, He Y, Karsdal M, Henrotin Y, Mobasheri A, Önnerfjord P, BayJensen A. The minor collagens in articular cartilage. Protein Cell. 2017 Aug;8(8):560- 572. doi: 10.1007/s13238-017-0377-7. Epub 2017 Feb 17. PMID: 28213717; PMCID: PMC5546929.
8. Gottardi R, Hansen U, Raiteri R, Loparic M, Düggelin M, Mathys D, Friederich NF, Bruckner P, Stolz M. Supramolecular Organization of Collagen Fibrils in Healthy and Osteoarthritic Human Knee and Hip Joint Cartilage. PLoS One. 2016 Oct 25;11(10):e0163552. doi: 10.1371/journal.pone.0163552. PMID: 27780246; PMCID: PMC5079628.
9. Eyre D. Collagen of articular cartilage. Arthritis Res. 2002;4(1):30-5. doi: 10.1186/ ar380. Epub 2001 Oct 5. PMID: 11879535; PMCID: PMC128915.
10. Penolazzi L, Pozzobon M, Bergamin LS, D'Agostino S, Francescato R, Bonaccorsi G, De Bonis P, Cavallo M, Lambertini E, Piva R. Extracellular Matrix From Decellularized Wharton's Jelly Improves the Behavior of Cells From Degenerated Intervertebral Disc. Front Bioeng Biotechnol. 2020 Mar 27;8:262. doi: 10.3389/fbioe.2020.00262. PMID: 32292779; PMCID: PMC7118204.
11. Xue M, Jackson CJ. Extracellular Matrix Reorganization During Wound Healing and Its Impact on Abnormal Scarring. Adv Wound Care (New Rochelle). 2015 Mar 1;4(3):119- 136. doi: 10.1089/wound.2013.0485. PMID: 25785236; PMCID: PMC4352699.
12. Velarde F, Castañeda V, Morales E, Ortega M, Ocaña E, Álvarez-Barreto J, Grunauer M, Eguiguren L, Caicedo A. Use of Human Umbilical Cord and Its Byproducts in Tissue Regeneration. Front Bioeng Biotechnol. 2020 Mar 10;8:117. doi: 10.3389/ fbioe.2020.00117. PMID: 32211387; PMCID: PMC7075856.
13. Kim N, Cho SG. Clinical applications of mesenchymal stem cells. Korean J Intern Med. 2013 Jul;28(4):387-402. doi: 10.3904/kjim.2013.28.4.387. Epub 2013 Jul 1. PMID: 23864795; PMCID: PMC3712145.
14. Navani A, Manchikanti L, Albers SL, Latchaw RE, Sanapati J, Kaye AD, Atluri S, Jordan S, Gupta A, Cedeno D, Vallejo A, Fellows B, Knezevic NN, Pappolla M, Diwan S, Trescot AM, Soin A, Kaye AM, Aydin SM, Calodney AK, Candido KD, Bakshi S, Benyamin RM, Vallejo R, Watanabe A, Beall D, Stitik TP, Foye PM, Helander EM, Hirsch JA. Responsible, Safe, and Effective Use of Biologics in the Management of Low Back Pain: American Society of Interventional Pain Physicians (ASIPP) Guidelines. Pain Physician. 2019 Jan;22(1S):S1-S74. PMID: 30717500.
15. CFR- Code of Regulations Title 21. US Food and Drug Administration. 2022.
16. Zhang Y, Liu S, Guo W, Wang M, Hao C, Gao S, Zhang X, Li X, Chen M, Jing X, Wang Z, Peng J, Lu S, Guo Q. Human umbilical cord Wharton's jelly mesenchymal stem cells combined with an acellular cartilage extracellular matrix scaffold improve cartilage repair compared with microfracture in a caprine model. Osteoarthritis Cartilage. 2018 Jul;26(7):954-965. doi: 10.1016/j.joca.2018.01.019. Epub 2018 Jan 31. PMID: 29391278.
17. Li Z, Bi Y, Wu Q, Chen C, Zhou L, Qi J, Xie D, Song H, Han Y, Qu P, Zhang K, Wu Y, Yin Q. A composite scaffold of Wharton's jelly and chondroitin sulphate loaded with human umbilical cord mesenchymal stem cells repairs articular cartilage defects in rat knee. J Mater Sci Mater Med. 2021 Mar 29;32(4):36. doi: 10.1007/s10856-021-06506-w. PMID: 33779853; PMCID: PMC8007499.
18. Sophia Fox AJ, Bedi A, Rodeo SA. The basic science of articular cartilage: structure, composition, and function. Sports Health. 2009 Nov;1(6):461-8. doi: 10.1177/1941738109350438. PMID: 23015907; PMCID: PMC3445147.
19. Majore I, Moretti P, Stahl F, Hass R, Kasper C. Growth and differentiation properties of mesenchymal stromal cell populations derived from whole human umbilical cord. Stem Cell Rev Rep. 2011 Mar;7(1):17-31. doi: 10.1007/s12015-010-9165-y. PMID: 20596801.
20. Sadlik B, Jaroslawski G, Puszkarz M, Blasiak A, Oldak T, Gladysz D, Whyte GP. Cartilage Repair in the Knee Using Umbilical Cord Wharton's Jelly-Derived Mesenchymal Stem Cells Embedded Onto Collagen Scaffolding and Implanted Under Dry Arthroscopy. Arthrosc Tech. 2017 Dec 25;7(1):e57-e63. doi: 10.1016/j.eats.2017.08.055. PMID: 29552470; PMCID: PMC5852271.
21. Gillies AR, Lieber RL. Structure and function of the skeletal muscle extracellular matrix. Muscle Nerve. 2011 Sep;44(3):318-31. doi: 10.1002/mus.22094. PMID: 21949456; PMCID: PMC3177172.
22. Csapo R, Gumpenberger M, Wessner B. Skeletal Muscle Extracellular Matrix - What Do We Know About Its Composition, Regulation, and Physiological Roles? A Narrative Review. Front Physiol. 2020 Mar 19;11:253. doi: 10.3389/fphys.2020.00253. PMID: 32265741; PMCID: PMC7096581.

Acknowledgements

The SEM images in this work were obtained at Montana Nanotechnology Facility, a member of the National Nanotechnology Coordinated Infrastructure (NNCI).